Energy Transfer from a Single Semiconductor Nanocrystal to Dye Molecules

Zheng Hua,[†] Qinfeng Xu,[†,‡] Xiangnan Huang,[†] Chunfeng Zhang,[†] Xiaoyong Wang,[†,*] and Min Xiao[†,⊥,*]

[†]National Laboratory of Solid State Microstructures and School of Physics, Nanjing University, Nanjing 210093, China, [‡]Department of Physics and Optoelectronic Engineering, Ludong University, Yantai 264025, China, and [⊥]Department of Physics, University of Arkansas, Fayetteville, Arkansas 72701, United States

ABSTRACT In an energy transfer (ET) process, it is the optical responses of donor and acceptor materials on the single-particle level that ultimately determine its overall performance. Here we conduct time-tagged, time-resolved optical measurements to correlate the photoluminescence (PL) intensities and lifetimes of a donor semiconductor nanocrystal (NC) and acceptor dye molecules linked to its surface. We reveal that the PL intensity of dye molecules follows exactly the blinking behavior of the donor NC and shows a step-like quenching behavior due to the photobleaching effect. The corresponding recovery of the NC PL intensity has allowed us to realize the textbook definition of PL quantum efficiency measurement in dye molecules upon absorbing a single exciton. Our theoretical fitting of the lifetime data demonstrates that the buildup time of acceptor PL could be solely determined by the radiative lifetime of dye molecules when it is any shorter than the NC lifetime, thus confirming the long-existing Förster theory on ET dynamics.

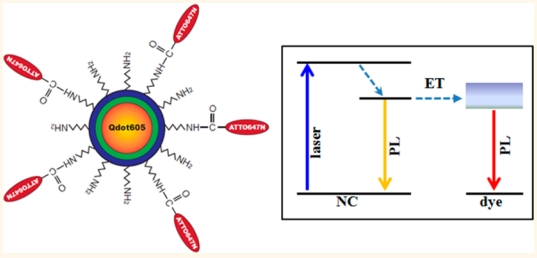

KEYWORDS: energy transfer · nanocrystal · single-particle · time-resolved

Förster resonance energy transfer (ET) represents a fundamental interaction between optical materials whereby the excitation energy can be effectively extracted from the donor to the acceptor by means of nonradiative dipole−dipole coupling.[1,2] For the device applications of ET, such as in energy harvesting,[3] light-emitting diodes,[4] and biosensing,[5,6] its efficiency (E) is the most important factor that is mainly determined by the spectral overlap between the donor emission and acceptor absorption profiles, as well as by their separation distance.[7,8] Experimentally, one only needs to measure $I_{DA}(\tau_{DA})$ and $I_D(\tau_D)$, corresponding to the donor fluorescence intensities (lifetimes) with and without the acceptor presence, and the ET efficiency can be directly calculated from either $E = 1 - I_{DA}/I_D$ or $E = 1 - \tau_{DA}/\tau_D$.[7,8] In principle, any efficient ET should be ultimately performed on the 1−10 nm length scale by a limited number of donors and acceptors, which dictates that a precise understanding of this process has to be achieved at the single-particle level to avoid the ensemble averaging effect. So far, this single-particle approach has been adopted to study ET mainly between semiconductor nanocrystals (NCs) and organic dye molecules,[5,9−15] with the research efforts being focused on the photoluminescence (PL) measurement of either the intensity[5,9−13] or the lifetime,[14] but rarely of both simultaneously on the same ET couple.[15] It would be interesting and of great importance to correlate these two PL parameters from a single ET couple for a complementary description of the ET process, a challenging task that has not yet been fulfilled ever since the ET mechanism was originally proposed in 1948.[16]

Here we conduct time-tagged, time-resolved optical measurements to correlate the PL intensities and lifetimes of a donor semiconductor NC and acceptor dye molecules linked to its surface. We reveal that the PL intensity of dye molecules follows exactly the blinking behavior of the donor NC and shows a step-like quenching behavior due to the photobleaching effect. The corresponding recovery of the NC PL intensity has allowed us to realize the textbook definition of PL quantum efficiency (QY) measurement in dye molecules upon

* Address correspondence to
(X. Wang)
wxiaoyong@nju.edu.cn,
(M. Xiao)
mxiao@uark.edu.

Received for review April 9, 2014
and accepted June 5, 2014.

Published online June 05, 2014
10.1021/nn5019736

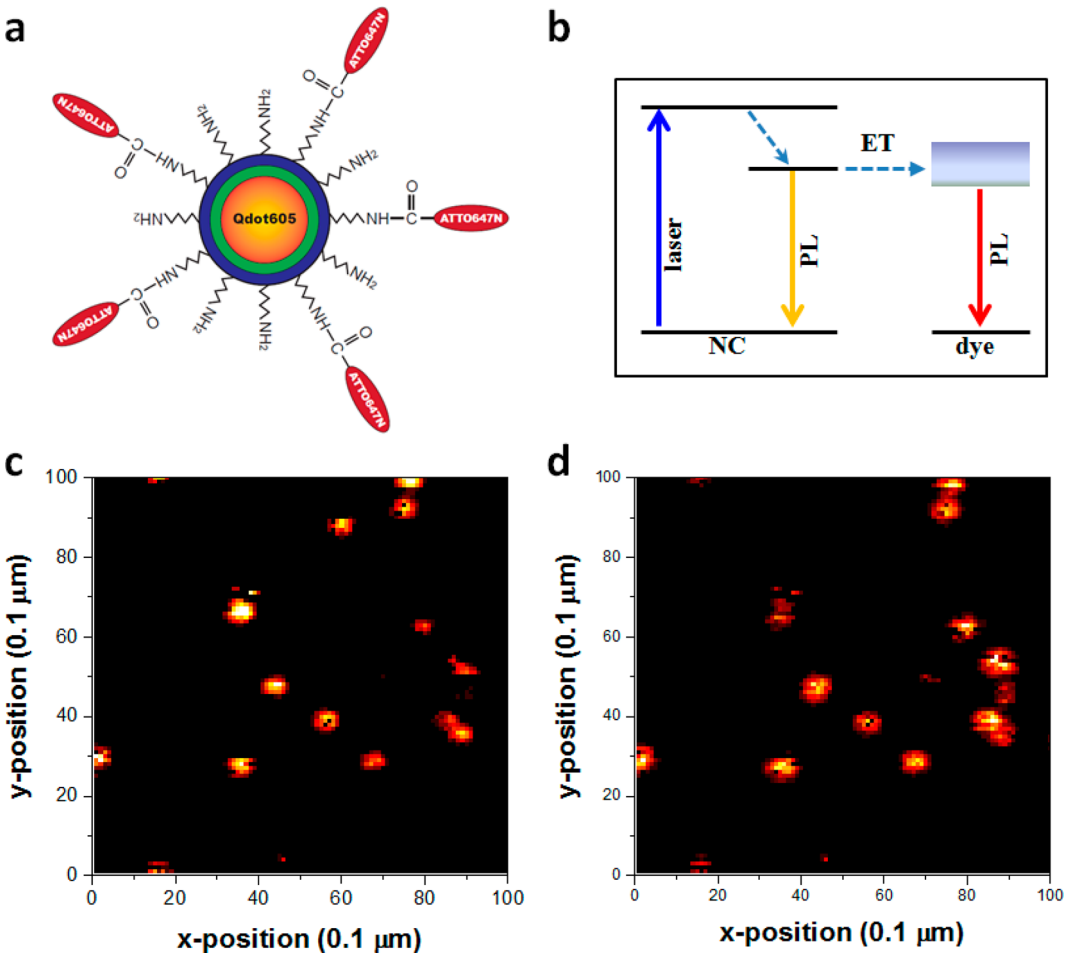

Figure 1. (a) Schematic diagram showing an ET particle composed of a single CdSe NC and several ATTO647N dyes linked to its surface. (b) Energy level structures of the donor NC and acceptor dyes involved in the ET process. Confocal scanning PL images of (c) the donor NCs and (d) the acceptor dyes obtained within the same sample area (10 μm × 10 μm).

absorbing a single exciton. Our theoretical fitting of the lifetime data demonstrates that the buildup time of acceptor PL could be solely determined by the radiative lifetime of dye molecules when it is any shorter than the NC lifetime, thus confirming the long-existing Förster theory on ET dynamics. Our findings also highlight the exciting possibility of transforming nonquantized optical emitters into a single-photon-emitting source by means of single-exciton ET from a semiconductor NC.

RESULTS AND DISCUSSION

We choose to covalently link to the surface of a single CdSe NC (Qdot605, from Life Technologies) a small ensemble of dye molecules (ATTO647N, from ATTO-TEC) to form a single donor−acceptors ET system (see Figure 1a and the Experimental Section). As shown in Figure S1 of the Supporting Information, the NC emission and dye absorption spectra overlap well with each other, and their emission spectra are almost completely separated to make isolation of their fluorescent photons at two different detectors easy. To minimize direct fluorescence from dye molecules, we excite a single ET particle at the laser wavelength of ~490 nm to first pump a single exciton to the NC absorption state (Figure 1b). After relaxing to the NC emitting state, this single exciton can either return to the NC ground state or be transferred to the surrounding dyes, leading to a single-photon emission in either case. This kind of sample configuration in Figure 1a, compared to others reported in literature that mixed NCs and dyes directly in a solid film[9,17] or connected them with one type of linker molecules,[5,6,10] features an abundance of acceptors brought in close proximity to a single donor so that a highly efficient ET process can be potentially realized.[11,18,19] This has provided us an unprecedented sensitivity to have a closer look at the ET process through correlated PL intensity and lifetime measurements on a single donor−acceptors couple.

In Figure 1c and d, we present two PL images for single NCs and their surface dyes, respectively, which were obtained by raster scanning a sample area (10 μm × 10 μm) through the laser focus of a confocal optical microscope and sending the PL signals onto two different detectors. In the location of each single NC

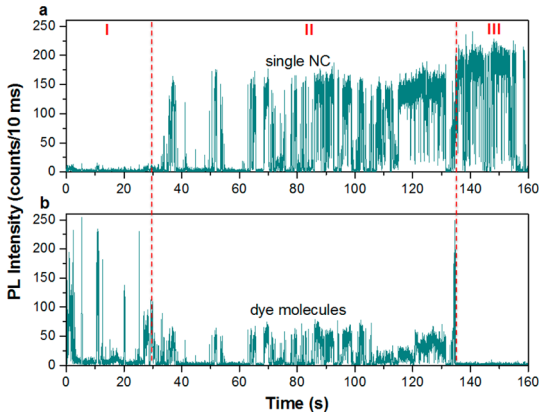

Figure 2. PL intensity *versus* time traces measured for (a) the donor NC and (b) the acceptor dyes, respectively. On the basis of the PL intensity variations, these two time traces are roughly divided by two vertical dashed lines into three stages of I, II, and III with decreasing ET efficiencies.

in Figure 1c, the fluorescence spot of its surface dyes can be clearly resolved in Figure 1d. Some bright NCs are correlated with dim dyes, or *vice versa*, implying an inhomogeneous distribution of the ET efficiencies possibly due to the number variation of available acceptor dyes on the NC surface. In Figure 2a and b, we have isolated a single ET particle and plotted the PL intensity *versus* time traces for the donor NC and its acceptor dyes, respectively. When the NC PL is "off", the dye photon counts fall within the detector background level, demonstrating that the signature of single NC PL blinking[20,21] is also transferred to its surrounding dyes.[9,10,13] A close examination of the PL intensity *versus* time traces of acceptor dyes shows that their PL intensity is always "on" ("off") as long as the donor NC is at the "on" ("off") PL period. This strongly implies that intrinsic PL blinking of ATTO647N dyes studied here is extremely weak, or it can be largely suppressed under such an ET-pumping condition. In the following ET studies, we will put emphasis only on the PL intensities and lifetimes measured during the blinking "on" time periods for both donor NC and acceptor dyes.

Nearly all of the single ET particles studied in our experiment (~39) showed one to four steps of discrete increase (decrease) in the NC (dye) PL intensity with the measurement time before the dye PL was completely bleached. We observed in only a few cases that the PL intensity change was associated with even more steps. The PL intensity *versus* time traces shown in Figure 2 were measured from a single ET particle with two steps of PL intensity change (see Figure S2 of the Supporting Information for another ET particle with a single step change of PL intensity). We can roughly divide the two time traces in Figure 2 into three stages denoted by I, II, and III, respectively. At stage I, the PL intensity (I_I^{nc}) of the donor NC is extremely weak, while that of the acceptor dyes possesses its maximum value. At stage II, some of the acceptor dyes are photobleached, bringing down their PL to a lower level, together with a

TABLE 1. PL Intensity and Lifetime Data for the Donor NC and Acceptor Dyes at Different ET Stages[a]

	NC		dyes		
stage	I^{nc} (counts/10 ms)	τ (ns)	I^{dye} (counts/10 ms)	τ_1 (ns)	τ_2 (ns)
I (0—30 s)	14	0.60	185	1.18	5.40
II (50—100 s)	136	9.55	50	5.47	9.55
III (140—160 s)	184	12.60	2.5		

[a] I^{nc} (I^{dye}): average photon count of "on"-period donor NC (acceptor dyes) calculated from those time bins with top 10% photon counts of each ET stage. τ: "on"-period PL decay lifetime of the donor NC obtained from a single-exponential fitting in Figure 4a. τ_1 and τ_2: "on"-period PL rising and decaying lifetimes of acceptor dyes obtained from a theoretical fitting with the summation of two exponential functions in Figure 4b.

significant increase of the donor NC PL (I_{II}^{nc}). At stage III, the dye PL is completely quenched and the NC regains its intrinsic PL intensity (I_{III}^{nc}) from purely radiative recombination. The PL intensities for the donor NC and acceptor dyes at three different stages of Figure 2 are listed in Table 1, from which the ET efficiencies can be calculated from $E_I = 1 - I_I^{nc}/I_{III}^{nc}$ and $E_{II} = 1 - I_{II}^{nc}/I_{III}^{nc}$ to be ~94.5% and ~26.0% for stages I and II, respectively. In Figure S3 of the Supporting Information, we plot a histogram for the distribution of ET efficiencies calculated from the initial and final PL intensities of the 39 single donor NCs studied in our experiment, showing the maximum ET efficiency that could be achieved in each single ET particle.

The step-like changes in the PL intensities of both donor NC and acceptor dyes in Figure 2 can be further demonstrated in Figure S4 of the Supporting Information, where we have plotted their intensity ratio as a function of the measurement time. Since the single ET particles are deposited on a solid substrate, the chance for the reorientation of single dye molecules would be small, although this possibility cannot be completely excluded. For all of the single ET particles studied, the dye PL would be exclusively quenched in the end, signifying the dominant influence of dye bleaching on the measured ET efficiencies. We surmise that reorientation of dye molecules might cause only random fluctuations in the ET efficiencies within each PL intensity level, as demonstrated by the NC/dyes PL intensity ratio plotted in Figure S4, instead of the almost irreversible decrease of ET efficiencies across discrete PL levels with the measurement time.

From the two PL intensity *versus* time traces in Figure 2, it is also possible for us to evaluate the PL QY of η for an ensemble of dye molecules upon absorption of a single NC exciton. For example, on the transition from stage II to III, the recovered PL intensity $I_{III}^{nc} - I_{II}^{nc}$ should arise from those NC excitons transferred at stage II to acceptor dyes with a PL intensity of I_{II}^{dye}. Then the dye PL QY at stage II can be calculated from $\eta = 0.772 I_{II}^{dye}/(I_{III}^{nc} - I_{II}^{nc})$ to be ~84.0%, where a factor of 0.772 is applied to take into account the

relative collection efficiencies between the NC and dye detectors. The dye PL QY at stage I with a PL intensity of I_I^{dye} can be similarly obtained from $\eta = 0.772(I_I^{dye} - I_{II}^{dye})/(I_{II}^{nc} - I_I^{nc})$ to be ~85.2%, implying that it almost keeps a constant value during these two ET processes. There may exist a variety of routine methods for the PL QY measurements of optical emitters, such as using integration spheres to count the input/output photons[22] and approximating excitation power density along with the sample absorption cross-section.[23] However, this single-particle ET approach taken here would be more powerful in that it can precisely estimate the probability for dyes to emit a photon after absorbing a single exciton/photon, a thought experiment that previously can be found only in the textbook definition.[7,8]

In Figure 3, we make a 2D plot to correlate the PL intensities of donor NC and acceptor dyes measured at each time point in Figure 2. A significant number of data points are grouped around the origin, which can be attributed to the missing emission of dyes when the NC is dwelling at its blinking "off" period. Another two clusters of data points can also be found whose center points B and C are linked to the origin with two green dashed lines. Cluster C should result from ET stage III in Figure 2 when the NC regains its maximum PL intensity after the dyes are completely photobleached, while cluster B is related to stage II with a small amount of dyes still surviving to extract NC excitons in the ET process. If we connect the center points of these two clusters (blue dashed line), the slope $k_1 = I_{II}^{dye}/(I_{III}^{nc} - I_{II}^{nc})$ of line CB should be equal to $\eta/0.772$, where η is the dye PL QY defined earlier in the text. In Figure 3, we can also observe that some data points are sparsely distributed along the green dashed line drawn near the vertical axis. These data points come from stage I in Figure 2 with an extremely high ET efficiency and should be centered at point A, where their distribution line intersects with the extension of line CB. However, since the number of blinking "on" durations at this stage is very limited and the NC PL intensity is hardly discerned from the background level, this clustering effect is not obvious despite that a positive correlation between the NC and dye PL intensities still exists. If we take cluster B (or stage II) as an example, the slope of its green line can be expressed as $k_2 = I_{II}^{dye}/I_{II}^{nc} = \eta E_{II}/[0.772(1 - E_{II})] = k_1 E_{II}/(1 - E_{II})$, from which we can estimate the ET efficiency of E_{II} at this stage. The above approach can also be applied to the other two clusters in Figure 3, and thus, one can get a very intuitive estimate of the ET efficiency by simply measuring two types of line slopes (k_1 and k_2) from such a 2D plot.

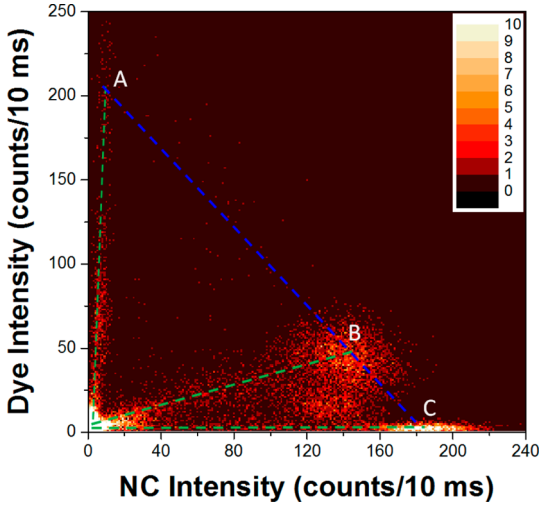

Figure 3. 2D plot for the correlated PL intensities of an ET particle. The bright spot around the origin corresponds to ET of the NC blinking "off" period, while clusters A, B, and C correspond to ET of the NC blinking "on" periods at stages I, II, and III, respectively. From the slopes of lines connecting the origin and points A, B, and C, as well as the line slope of CB, the ET efficiencies of stages I, II, and III can be intuitively obtained.

The PL intensity *versus* time traces in Figure 2 were acquired from the time-tagged time-resolved (TTTR) measurements (see Experimental Section), which allowed us to obtain PL lifetimes for both the NC and dye molecules at the three ET stages. As shown in Figure 4a, the NC PL always has a single-exponential decay with lifetime values of ~0.60, ~9.55, and 12.60 ns for stages I, II, and III, respectively. The PL decay lifetime measured

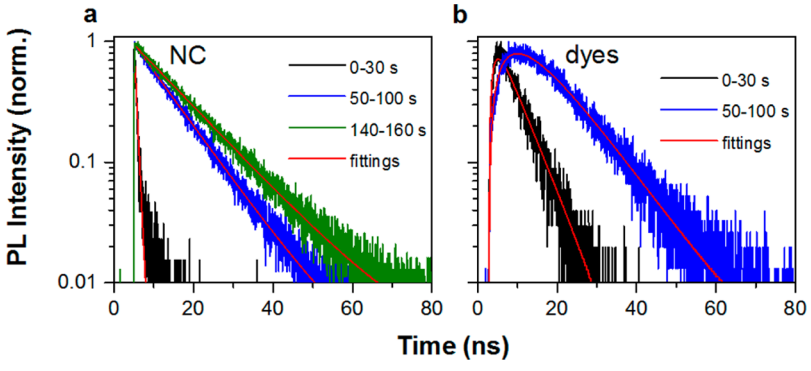

Figure 4. (a) Transient PL curves measured for the "on"-period intensities of donor NC at stages I (0–30 s), II (50–100 s), and III (140–160 s), respectively. The decaying part for each of the three curves is fitted with a single exponential function (red line). (b) Transient PL curves measured for the "on"-period intensities of acceptor dyes at stages I (0–30 s) and II (50–100 s), respectively. Each of these two curves is fitted by the summation of two exponential functions (red line).

at stage III (τ_{III}^{nc}) should come directly from radiative recombination (τ_{rad}^{nc}) of single NC excitons without any ET influence (see the Supporting Information, Figure S5). Then the ET efficiencies at stages I and II can be calculated from $E_I = 1 - \tau_I^{nc}/\tau_{III}^{nc}$ and $E_{II} = 1 - \tau_{II}^{nc}/\tau_{III}^{nc}$ to be ~95.2% and ~24.2%, respectively, which agree well with those values deduced from the PL intensity measurements in Figure 2a. Given the fact that the PL decay rates of NC at stages I and II can be expressed as $k_I^{nc} = 1/\tau_I^{nc} = 1/\tau_{rad}^{nc} + 1/\tau_I^{ET}$ and $k_{II}^{nc} = 1/\tau_{II}^{nc} = 1/\tau_{rad}^{nc} + 1/\tau_{II}^{ET}$, we can calculate their ET lifetimes of τ_I^{ET} and τ_{II}^{ET} to be ~0.63 and ~39.45 ns, respectively. This relatively large dynamic range clearly shows the influence of the number of available acceptors on the ET lifetime from a single-particle point of view.

In Figure 4b, we also plot the transient PL curves measured for acceptor dyes where both the rising and decaying parts are relatively slower at stage II than those at stage I. To properly assign the origins for the rising and decaying components, we turn to a model proposed from the Förster theory.[7] At a given time point of t', the probability density for a single exciton to be present in the NC would be $I^{nc}(t') \propto e^{-k^{nc}t'}$, where $k^{nc} = 1/\tau^{nc}$ is the total PL decay rate of the NC already defined earlier in the text for both stages I and II. At t' and with an ET efficiency of E, this exciton would be transferred to dye molecules and decay with their radiative rate of $k^{dye} = 1/\tau^{dye}$. Then the probability for dye molecules to emit a photon at the time point of t should be $I^{nc}(t')I^{dye}(t - t')$, which is proportional to $e^{-k^{nc}t'}e^{-k^{dye}(t - t')}$. Now we can vary t' from 0 to t for the integration, and the transient PL of dye molecules is finally obtained as $I^{dye}(t) \propto (-e^{-k^{nc}t} + e^{-k^{dye}t})/(k^{nc} - k^{dye})$. In the numerator of this formula, there are two exponential functions that can switch signs according to the relative values of k^{nc} and k^{dye} in the denominator, with positive (negative) sign corresponding to the decaying (rising) part of the transient PL.

As shown in Figure 4b, each of the two transient PL curves is fitted by $A(-e^{-t/\tau_1} + e^{-t/\tau_2})$ with A being a positive constant, and the rising and decaying lifetimes of τ_1 and τ_2 are listed in Table 1. At stage I, the NC PL lifetime of ~0.60 ns is almost completely dominated by the nonradiative ET process. In Figure 4b, the transient PL curve measured at this stage has a decaying constant of τ_2 = ~5.4 ns, which we attribute to radiative recombination of solid-phase dye molecules, although it deviates to some degree from the ~4.70 ns value measured in solution (see the Supporting Information, Figure S6). Meanwhile, the rising lifetime of τ_1 = ~1.18 ns is a little longer than the NC lifetime of ~0.60 ns, and this discrepancy can be mainly explained by different timing resolutions of the dye and NC detectors used in our experiment (see Experimental Section and the Supporting Information, Figure S7). It should be noted that the "on"-period PL intensity at stage I of Figure 2a is only slightly higher than that of the "off"-period, which is caused by carrier channeling into the NC intrinsic traps and possibly additional traps introduced by the attachment of dye molecules.[15] Then unavoidable inclusion of the "off" time bins may also contribute to the shortened "on"-period PL decay lifetime of donor NC relative to the PL rise time of acceptor dyes. At stage II when the NC lifetime of ~9.55 ns is longer than the dye radiative lifetime of ~5.40 ns, it can be clearly seen from Table 1 that they do perfectly take over the decaying (τ_2 = ~9.55 ns) and rising (τ_1 = ~5.47 ns) parts of dye transiet PL, respectively. In nearly all previous ET studies employing time-resolved measurements, the influence of ET on acceptor PL dynamics was exclusively directed to the rising part,[24,25] and only in rare cases was it discovered that the decaying part might also be altered.[14] Here, for the first time, we have experimentally confirmed a long-existing prediction of Förster theory[7] that necessitates a wise comparison between the donor and acceptor lifetimes for a better understanding and control of the ET dynamics.

CONCLUSIONS

To summarize, we have performed TTTR optical measurements on a single ET couple composed of a donor semiconductor NC and an ensemble of acceptor dyes linked to its surface. This allows us to make correlated PL intensity and lifetime measurements on the donor and acceptors that yield similar ET efficiencies. On the basis of the PL intensity data, we have estimated the PL QY of dye molecules upon absorbing a single exciton. On the basis of the PL lifetime data, we have demonstrated that the rising and decaying parts of acceptor PL could be determined by the dye radiative lifetime and the NC lifetime, respectively, when the former is any shorter than the latter. We believe that the above findings would greatly deepen the current understanding of the ET process to benefit a variety of its device applications in energy harvesting, light-emitting diodes, biosensing, and quantum optics. Specifically, the quantized NC transfers only a single exciton to the dye ensemble at a given time (see the Supporting Information, Figure S8), which highlights the exciting possibility of transforming nonquantized optical emitters into a single-photon-emitting source by means of single-exciton ET from a semiconductor NC.

EXPERIMENTAL SECTION

Sample Preparations. The ATTO647N dyes modified with NHS-ester (MW: 834 g/mol) and the Qdot605 ITK amino (PEG) NCs were purchased from ATTO-TEC and Life Technologies, respectively. The solution CdSe NCs, with a concentration of 8 μM, are functionalized with amine-derivatized PEGs on the surface,

which can react efficiently with NHS-ester.[26] The average number of PEGs on the surface of each NC is ~40−60,[27] which sets a maximum limit for the number of acceptor dyes that can be attached. A 15 μL amount of the NC solution was added to a 200 μL buffer of 0.1 M sodium bicarbonate (pH 8.3) containing 0.1 mg of ATTO647N dyes. The ratio between the NC and dye concentrations in the buffer was estimated to be ~1:500. The NC−dye mixture was incubated for 2 h at room temperature with continuous stirring, after which unreacted dyes were filtered out by a 30 K MWCO VivaSpin device (Sartorius) centrifuging the column for 15 min at 14000*g*. According to ref 1, the Förster radius of the Qdot605-ATTO647N ET particle can be calculated to be ~6.5 nm, as compared to a diameter distribution of 10−15 nm for the single Qdot605 NCs.[28]

Estimation of the Number of Dye Molecules. As mentioned above, the maximum number of dye molecules on each single NC should be ~40−60, which is mainly set by the available PEGs on the NC surface that can react with the NHS-ester of dye molecules. Since only a step-like increase (decrease) of the NC (dye) PL intensity was observed from these single ET particles studied in our experiment, we believe that the average number of dye molecules on each single NC is far less than ~40−60, in which case we would expect a continuous change of the PL intensity during the dye-bleaching process. Here we adopt a method reported in ref 29 to count the number of dye molecules linked to the surface of a single NC from the intensity values of their discrete PL levels. We first assume a homogeneous distribution of dye molecules on the NC surface with the same ET efficiency. We further assume that their PL intensity level measured right before permanent bleaching should originate from a single dye molecule. Then the intensity ratio between their first and last PL levels in a PL intensity *versus* time trace would roughly reflect the number of dye molecules linked to the surface of a single NC. As shown in Figure S9 of the Supporting Information, the occurrence counts of such dye PL intensity ratios from 39 single ET particles are plotted, from which the number of dye molecules on the surface of each single NC can be estimated to be from ~2 to 8. It should be pointed out that there still exist some uncertainties in estimating the number of dye molecules from the data shown in Figure S9. For example, if the dye molecules are not homogeneously distributed, the bleaching of a dye molecule with a higher ET efficiency would result in a larger decrease of the dye PL intensity and, thus, an overestimate of the number of dye molecules. However, if some of the dye molecules have already been bleached before the PL intensity *versus* time trace measurement, the number of dye molecules would be underestimated from the data shown in Figure S9.

Optical Characterizations. One drop of the as-prepared sample solution was spin-casted onto a fused silica coverslip to form a solid film for the optical characterizations at room temperature. The 490 nm output of a 7.8 MHz, picosecond supercontinuum fiber laser (EXR-15, NKT Photonics) was used as the excitation source to avoid direct fluorescence of acceptor dyes. The laser beam was set at a power density of ~20 W/cm^2 and focused onto the sample substrate by a 100× immersion-oil objective. The sample substrate was loaded onto a home-built confocal scanning optical microscope with a stepping resolution of 200 nm and a dwell time of 200 ms. The PL signal of a single ET particle was collected by the same objective and sent through a beamsplitter tube to two avalanche photo diodes (APDs) in a time-correlated single-photon counting (TCSPC) system. A band-pass filter was placed before each of these two APDs to detect the NC and dye photons separately, with a relative collection efficiency of ~0.772. The NC APD (PDM-APD, PicoQuant) and dye APD (Tau-SAPD, PicoQuant) have timing resolutions of 0.492 and 0.832 ns, respectively, as measured from the scattered excitation laser photons (see the Supporting Information, Figure S7). The TCSPC system was operated under the TTTR mode so that the arrival times of each photon relative to the laboratory time and the laser pulse time could be obtained, which allowed us to plot the PL intensity *versus* time traces and transient PL curves, respectively. The "on"-period transient PL curves of donor NC and acceptor dyes were plotted and analyzed by the SymPhoTime software from PicoQuant.

Conflict of Interest: The authors declare no competing financial interest.

Acknowledgment. This work is supported by the National Basic Research Program of China (Nos. 2012CB921801 and 2011CBA00205), the National Natural Science Foundation of China (Nos. 91021013, 91321105, 11274161, 11321063, and 61307067), the New Century Excellent Talents program (NCET-11-0238), Jiangsu Provincial Funds for Distinguished Young Scientists (No. BK20130012), the 333 Project Foundation of Jiangsu Province, the PAPD of Jiangsu Higher Education Institutions, and the Innovation Project of Graduate Student of Jiangsu Province (CXLX12_0034).

Supporting Information Available: Absorption and emission spectra of solution NCs and dyes, PL intensity *versus* time traces of a single ET particle, statistics for the distribution of maximum ET efficiencies from 39 single ET particles, NC/dyes PL intensity ratio as a function of the measurement time for a single ET particle, PL intensity *versus* time trace and PL decay curve of a single NC, PL decay curve of solution dyes, instrumental response functions of APDs, second-order photon correlation function of a single NC, and occurrence counts for the intensity ratios between the first and last PL levels of acceptor dyes in 39 single ET particles. This material is available free of charge *via* the Internet at http://pubs.acs.org.

REFERENCES AND NOTES

1. Clapp, A. R.; Medintz, I. L.; Mattoussi, H. Förster Resonance Energy Transfer Investigations Using Quantum-Dot Fluorophores. *ChemPhysChem* **2006**, *7*, 47–57.
2. Rogach, A. L.; Klar, T. A.; Lupton, J. M.; Meijerink, A.; Feldmann, J. Energy Transfer with Semiconductor Nanocrystals. *J. Mater. Chem.* **2009**, *19*, 1208–1221.
3. Buhbut, S.; Itzhakov, S.; Tauber, E.; Shalom, M.; Hod, I.; Geiger, T.; Garini, Y.; Oron, D.; Zaban, A. Built-in Quantum Dot Antennas in Dye-Sensitized Solar Cells. *ACS Nano* **2010**, *4*, 1293–1298.
4. Achermann, M.; Petruska, M. A.; Kos, S.; Smith, D. L.; Koleske, D. D.; Klimov, V. I. Energy-Transfer Pumping of Semiconductor Nanocrystals Using an Epitaxial Quantum Well. *Nature* **2004**, *429*, 642–646.
5. Zhang, C.-Y.; Yeh, H.-C.; Kuroki, M. T.; Wang, T.-H. Single-Quantum-Dot-Based DNA Nanosensor. *Nat. Mater.* **2005**, *4*, 826–831.
6. Medintz, I. L.; Clapp, A. R.; Mattoussi, H.; Goldman, E. R.; Fisher, B.; Mauro, J. M. Self-Assembled Nanoscale Biosensors Based on Quantum Dot FRET Donors. *Nat. Mater.* **2003**, *2*, 630–638.
7. Valeur, B. *Molecular Fluorescence: Principles and Applications*; Wiley-VCH: Weinheim, 2002.
8. Lakowicz, J. R. *Principles of Fluorescence Spectroscopy*, 2nd ed.; Plenum: New York, 1999.
9. Becker, K.; Lupton, J. M.; Müller, J.; Rogach, A. L.; Talapin, D. V.; Weller, H.; Feldmann, J. Electrical Control of Förster Energy Transfer. *Nat. Mater.* **2006**, *5*, 777–781.
10. Potapova, I.; Mruk, R.; Hübner, C.; Zentel, R.; Basché, T.; Mews, A. CdSe/ZnS Nanocrystals with Dye-Functionalized Polymer Ligands Containing Many Anchor Groups. *Angew. Chem., Int. Ed.* **2005**, *44*, 2437–2440.
11. Hohng, S.; Ha, T. Single-Molecule Quantum-Dot Fluorescence Resonance Energy Transfer. *ChemPhysChem* **2005**, *6*, 956–960.
12. Ren, T.; Mandal, P. K.; Erker, W.; Liu, Z.; Avlasevich, Y.; Puhl, L.; Müllen, K.; Basché, T. A Simple and Versatile Route to Stable Quantum Dot-Dye Hybrids in Nonaqueous and Aqueous Solutions. *J. Am. Chem. Soc.* **2008**, *130*, 17242–17243.
13. Gerlach, F.; Täuber, D.; von Borczyskowski, C. Correlated Blinking *via* Time Dependent Energy Transfer in Single CdSe Quantum Dot-Dye Nanoassemblies. *Chem. Phys. Lett.* **2013**, *572*, 90–95.
14. Soujon, D.; Becker, K.; Rogach, A. L.; Feldmann, J.; Weller, H.; Talapin, D. V.; Lupton, J. M. Time-Resolved Förster Energy

Transfer from Individual Semiconductor Nanoantennae to Single Dye Molecules. *J. Phys. Chem. Lett.* **2007**, *111*, 11511–11515.
15. Kowerko, D.; Schuster, J.; Amecke, N.; Abdel-Mottaleb, M.; Dobrawa, R.; Wurthner, F.; von Borczyskowski, C. FRET and Ligand-Related NON-FRET Processes in Single Quantum Dot-Perylene Bisimide Assemblies. *Phys. Chem. Chem. Phys.* **2010**, *12*, 4112–4123.
16. Förster, T. Intermolecular Energy Migration and Fluorescence. *Ann. Phys. (Berlin, Ger.)* **1948**, *2*, 55–75.
17. Zhang, Q.; Atay, T.; Tischler, J. R.; Bradley, M. S.; Bulović, V.; Nurmikko, A. V. Highly Efficient Resonant Coupling of Optical Excitations in Hybrid Organic/Inorganic Semiconductor Nanostructures. *Nat. Nanotechnol.* **2007**, *2*, 555–559.
18. Funston, A. M.; Jasieniak, J. J.; Mulvaney, P. Complete Quenching of CdSe Nanocrystal Photoluminescence by Single Dye Molecules. *Adv. Mater.* **2008**, *20*, 4274–4280.
19. Dworak, L.; Matylitsky, V. V.; Ren, T.; Basché, T.; Wachtveitl, J. Acceptor Concentration Dependence of Förster Resonance Energy Transfer Dynamics in Dye-Quantum Dot Complexes. *J. Phys. Chem. C* **2014**, *118*, 4396–4402.
20. Dabbousi, B. O.; Bawendi, M. G.; Macklin, J. J.; Trautman, J. K.; Harris, T. D.; Brus, L. E. Fluorescence Intermittency in Single Cadmium Selenide Nanocrystals. *Nature* **1996**, *383*, 802–804.
21. Michler, P.; Imamoğlu, A.; Mason, M. D.; Carson, P. J.; Strouse, G. F.; Buratto, S. K. Quantum Correlation Among Photons from a Single Quantum Dot at Room Temperature. *Nature* **2000**, *406*, 968–970.
22. Timmerman, D.; Valenta, J.; Dohnalová, K.; de Boer, W. D. A. M.; Gregorkiewicz, T. Step-Like Enhancement of Luminescence Quantum Yield of Silicon Nanocrystals. *Nat. Nanotechnol.* **2011**, *6*, 710–713.
23. Carlson, L. J.; Maccagnano, S. E.; Zheng, M.; Silcox, J.; Krauss, T. D. Fluorescence Efficiency of Individual Carbon Nanotubes. *Nano Lett.* **2007**, *7*, 3698–3703.
24. Achermann, M.; Petruska, M. A.; Crooker, S. A.; Klimov, V. I. Picosecond Energy Transfer in Quantum Dot Langmuir-Blodgett Nanoassemblies. *J. Phys. Chem. B* **2003**, *107*, 13782–13787.
25. Wang, X.; Shih, C.-K.; Xu, J.; Xiao, M. Enhanced Dipole-Dipole Interaction of CdSe/CdS Nanocrystal Quantum Dots inside a Planar Microcavity. *Appl. Phys. Lett.* **2006**, *89*, 113114.
26. Nikiforov, T. T.; Beechem, J. M. Development of Homogeneous Binding Assays Based on Fluorescence Resonance Energy Transfer between Quantum Dots and Alexa Fluor Fluorophores. *Anal. Biochem.* **2006**, *357*, 68–76.
27. Mittal, R.; Bruchez, M. P. Biotin-4-Fluorescein Based Fluorescence Quenching Assay for Determination of Biotin Binding Capacity of Streptavidin Conjugated Quantum Dots. *Bioconjugate Chem.* **2011**, *22*, 362–368.
28. Gunsolus, I. L.; Hu, D.; Mihai, C.; Lohse, S. E.; Lee, C.; Torelli, M. D.; Hamers, R. J.; Murhpy, C. J.; Orr, G.; Haynes, C. L. Facile Method to Stain the Bacterial Cell Surface for Super-Resolution Fluorescence Microscopy. *Analyst* **2014**, *139*, 3174–3178.
29. Trenkmann, I.; Bok, S.; Korampally, V. R.; Gangopadhyay, S.; Graaf, H.; von Borczyskowski, C. Counting Single Rhodamine 6G Dye Molecules in Organosilicate Nanoparticles. *Chem. Phys.* **2012**, *406*, 41–46.